J. Membrane Biol. 154, 69–79 (1996)

The Journal of
Membrane
Biology

Ionic Channels of the Sugar Beet Tonoplast are Regulated by a Multi-ion Single-file Permeation Mechanism

F. Gambale, M. Bregante, F. Stragapede, A.M. Cantu′
Istituto di Cibernetica e Biofisica, Via DeMarini 6, I-16149, Genova, Italy

Received: 26 December 1995/Revised: 10 July 1996

Abstract. Ionic channels of the sugar beet tonoplast were studied using the patch-clamp technique. At micromolar concentrations of cytosolic calcium, several (at least four) distinct single-channel current levels were routinely identified. On the basis of channel voltage dependence, kinetic properties and conductance of single openings, the largest channel (103 ± 2 pS in symmetric 150 mM KCl) corresponds to the slow vacuolar (SV) channel already identified by Hedrich and Neher (1987). The majority of the whole-vacuole current was ascribed to this time-dependent slow-activating channel elicited by positive vacuolar potentials. The channel of intermediate amplitude (41 ± 1 pS in 150 mM KCl) did not show any voltage dependence and delay in the activation upon the application of voltage steps to both positive and negative transmembrane potentials. Owing to its voltage independence this channel was denominated FV1. The opening probability of the SV-type channel increased by increasing the cytoplasmic calcium concentration, while the activity of the FV1 channel did not increase appreciably by changing the calcium concentration in the range from 6 μM to 1 mM. All the channels identified showed a linear current-voltage characteristic in the range ±100 mV and at least the three most conductive ones displayed potassium selectivity properties. Substitution of potassium with tetramethylammonium (TMA) on the cytosolic side demonstrated that both the SV and FV1 channels are impermeable to TMA influx into the vacuole and support the potassium selectivity properties of these two channels. Moreover, the single channel conductances of all the channels identified increased as a function of the potassium concentration and reached a maximum conductivity at $[K^+]$ ~0.5 M. This behavior can be explained by a multi-ion occupancy single-file permeation mechanism.

Key words: Ion channels — Vacuole — Sugar beet — Multi-ion pore — Single-file diffusion

Introduction

In plant vacuoles, the ionic current mediated by potassium channels has a main component with slow kinetics of activation at positive transmembrane voltages and no inactivation. The majority of the ion fluxes is mediated by the voltage-dependent SV (*S*low *V*acuolar) channel (Hedrich & Neher, 1987), however instantaneous FV (*F*ast *V*acuolar) channels and other channels of smaller amplitudes have also been observed (Coyaud et al., 1987; Hedrich & Neher, 1987; Kolb et al. 1987; Maathuis & Prins, 1991; Schulz-Lessdorf & Hedrich, 1995). It has been shown that an increase of the cytoplasmic calcium concentration (⩾0.1 μM) increases the opening probability of the SV channel, while the FV channel is active at nanomolar concentrations of cytoplasmic calcium (Hedrich & Neher, 1987). So far other investigators have carried out detailed studies only on the SV-type channel since the FV channel was labile and affected by a fast rundown within a few minutes from the excision of the patch (Hedrich & Neher, 1987). More recently, another fast activating channel (denominated VK), active at micromolar concentrations of cytoplasmic calcium (Ward & Schroeder, 1994), was characterized in guard cell vacuoles. Divalent selective channels with a slow kinetics of activation (Pantoja et al., 1992) and calcium-selective channels which exhibited fast kinetics of activation were also identified (Johannes et al., 1992; Johannes & Sanders, 1995) in tonoplasts from sugar beet cell-culture and tap roots, respectively.

Correspondence to: F. Gambale

Under our experimental conditions (6 μM cytoplasmic calcium), a voltage independent channel was usually very stable and could be routinely observed in the same patch together with the SV channel and with other channels of smaller amplitudes. We performed a detailed characterization of these channels comparing their properties under identical experimental conditions.

Materials and Methods

Sugar beet plants were grown either in the field or in the green house. Vacuoles were directly extruded into the recording chamber by cutting a slice of fresh taproot tissue and rinsing the surface with a few drops of bathing solution. The tonoplast ionic transport properties were studied using the patch-clamp technique either in the whole-vacuole or in the excised-patch and the vacuole-attached configurations. Access to the vacuole interior was gained by breaking the membrane under the patching pipette with short (1 msec) voltage pulses up to ~1V.

Transmembrane-voltage and ionic current were controlled and monitored with a List EPC7 current-voltage amplifier interfaced with an Instrutech A/D/A board (Instrutech, Elmont, NY). An Atari 4MegaST personal computer was used to generate the stimulation protocol and to store the digitized current record on the computer hard disk. Single-channel recordings were also stored on a videocassette recorder equipped with a PCM Sony F1, modified according to Bezanilla (1985). Current records were low-pass filtered with a 4-pole filter KemoVBF8 (Kemo, Beckenham, UK). Analysis of single channels were performed offline both on the Atari personal computer and in a 486 MS-DOS compatible system. Single-channel openings were individually recognized by using the commercial software TAC (Instrutech, Elmont, NY) or by constructing current histograms that were fit with theoretical Gaussian distributions. Channels could be unequivocally identified as belonging to one of the four families on the basis of their current amplitude, as well as on their activation and kinetic properties.

The standard bath solution was (in mM): KCl = 150, $MgCl_2$ = 2, HEPES = 5, adjusted to pH 7.1 by KOH (~5 mM), $CaCl_2$ = 0.97, EGTA = 1, resulting in cytosolic-free calcium concentration of 6 μM (according to Fabiato & Fabiato, 1979). The standard pipette solution was (in mM): KCl = 150, $CaCl_2$ = 1, $MgCl_2$ = 2, MES = 25, adjusted to pH 6.1 by KOH (~5 mM). To study the single channel conductance as a function of ionic concentration, distinct experiments were performed in standard solutions where the symmetric KCl concentration ranged between 50 mM and 1 M, while the osmotic pressure was adjusted to the tap root osmolarity by adding an appropriate amount of sorbitol.

Ionic solution in the bath was changed either by a fast (a few seconds) or by a slow (a few minutes) superfusion procedure. In the first case, two pipettes (one containing the bath control solution and the other containing the solution to be tested) were alternatively positioned in front of the vacuole, while the bath control solution in the Petri dish was continuously renewed using a peristaltic pump. In the second case, the bath solution was changed by means of the peristaltic pump.

All quoted potentials refer to the pipette (Bertl et al., 1992), (*see* the inset of Fig. 1), which means that the transmembrane potential across the vacuole is defined as the potential difference between the cytoplasmic and the lumen (out)side (Schulz-Lessdorf & Hedrich, 1995), i.e.:

$$V = V_{cytosol} - V_{vacuole}, \text{ where } V_{vacuole} = 0.$$

This implies that in the outside-out configuration positive or outward currents through the tonoplast represent a cation flow out of the cytosol into the vacuole.

The liquid junction potentials (LJP) were measured following the procedure described by Neher (1992) (*see also* Ward & Schroeder, 1994). In brief, an agar bridge containing 3 M KCl was the bath electrode, while the pipette electrode was filled with the pipette solution to be tested. In the current-clamp mode the voltage was adjusted to zero, then the pipette and bath electrodes were moved to a second chamber containing the bath solution. In our experimental conditions the LJP was read as the zero-current potential and we verified that it was always less than 1 mV. We also proved that the LJP did not change by varying the concentration of sorbitol currently used to adjust the osmotic pressure of the solution to that of the sugar beet. Nernst potentials and conductance versus activity were calculated taking into account the activity coefficient of the ionic solutions (Robinson & Stokes, 1959).

Results

Macroscopic Whole-vacuole Currents

In the whole-vacuole configuration the majority of the current of the sugar beet tonoplasts was usually mediated by the slow activating ($t_{1/2}$ ~ 500 msec) SV channel. The SV channel activated slowly after the application of positive potentials and did not inactivate, as demonstrated by positive pulses lasting several seconds; at negative potentials the channel deactivated within a few tens of msecs and displayed a very low opening probability (Hedrich & Neher, 1987). These properties are summarized in Fig. 1, where typical macroscopic currents, and the corresponding steady-state current-voltage characteristic (panel *B*), show that currents of several nanoamperes could be measured at positive potentials, while almost no current was detected at negative voltages.

In symmetric solutions, the time constant of the deactivating tail currents was systematically fitted by a single exponential function. Fig. 1*C* shows that the kinetics of deactivation of tail currents (at $V = -100$ mV) became slower when the amplitude of the step potential eliciting the outward (of the cytoplasm) current was increased; as a consequence double pulse protocols can be used to determine SV macroscopic and single-channel characteristics over a wide range of potentials. The *I-V* characteristic of the instantaneous tail current, measured in symmetric $MgCl_2$ = 5 mM (or $MgCl_2$ = 2 mM as in Fig. 1*D*) and asymmetric KCl (KCl_{In} = 150 mM, KCl_{Out} = 30 mM, other conditions as in standard solutions) indicates that the SV channel is selective for K^+. However, the difference between V_{rev} (+24 ± 1 mV, mean ± SEM, $N = 8$) and the Nernst potential for K^+ (+36.1 mV) suggests that the SV channel is not absolutely selective for K^+. Indeed, when the cytosolic $MgCl_2$ concentration was decreased from 5 mM to 0.2 mM, the reversal potential shifted to +35 ± 1 mV (mean ± SEM, $N = 8$), which implies that the SV channel is selective not only for K^+ but also for Mg^{2+} ions.

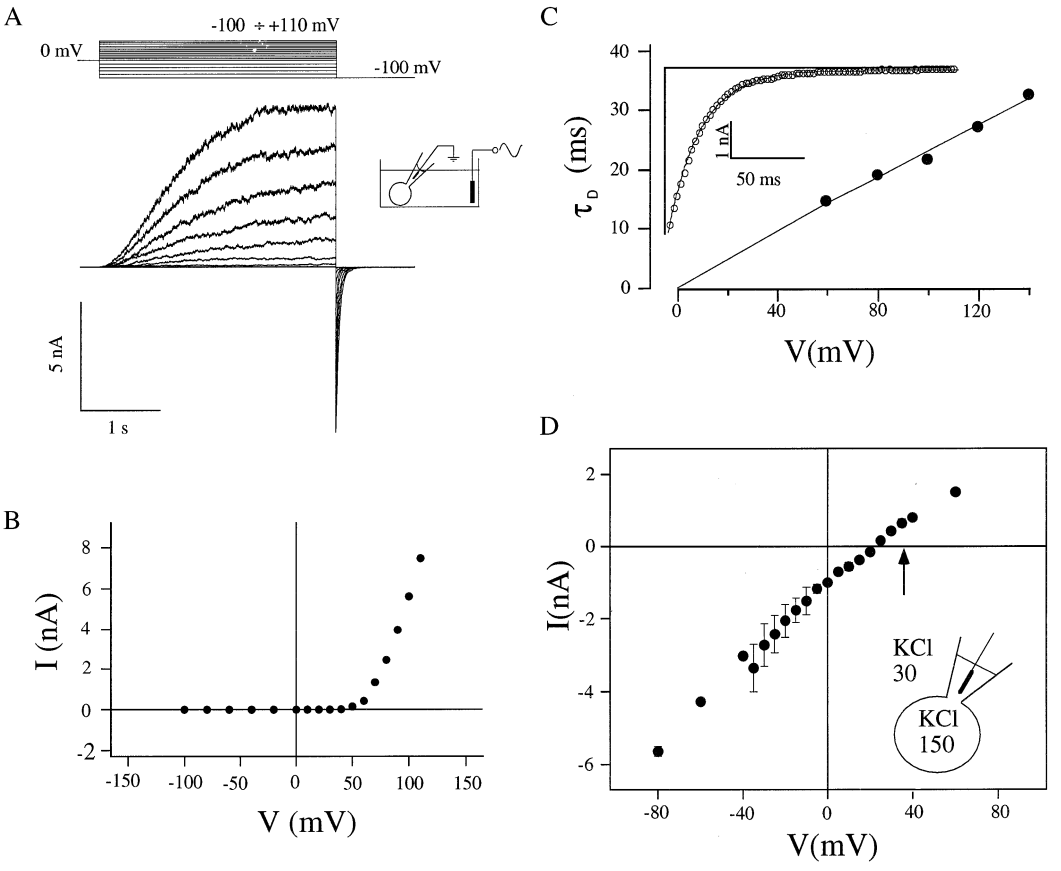

Fig. 1. Characteristic of the SV channel in sugar beet vacuoles. (*A*) Macroscopic whole-vacuole currents elicited by a series of voltage steps (represented in the upper inset) ranging from −100 to 0 mV in 20 mV steps, and from 0 to 110 mV in 10 mV steps. Holding and tail potentials were 0 and −100 mV, respectively. (*B*) Current-voltage characteristic (of data in *A*) obtained by plotting the steady state current at each test pulse. (*C*) The decay time, τ_D, measured at Vtail = −100 mV is plotted as a function of the step potential (filled symbols). Each point represents the mean value obtained from at least three records of the same experiment. *Inset:* every sixth data point (empty symbols) of a typical tail current is shown together with the best fit obtained by a single exponential function (continuous line). Data shown in *A, B* and *C* were obtained in standard ionic solutions. (*D*) Current-voltage relationship measured from instantaneous tail currents in asymmetric solutions. The bath solution contained (in mM): KCl 30, $MgCl_2$ 2, HEPES 5, adjusted to pH 7.1 by KOH 18.5 mM, $CaCl_2$ 0.97, EGTA 1; the standard pipette solution was (in mM): KCl 150, $CaCl_2$ 1, $MgCl_2$ 2, MES 25, adjusted to pH 6.1 by KOH 5 mM. Data are the results obtained from six different series of stimulations, mean ± SD.

Other Channels Colocalize with the SV Type

Despite the fact that the tonoplast current was dominated by the SV channel, other channel types contribute to the vacuolar currents as shown in Fig. 2 where different single-channel transitions present in the same patch are represented. Single-channel openings showing different kinetics and amplitudes can be clearly distinguished. The largest transitions, present at positive voltages in each record of Fig. 2, correspond to the SV channel since these openings were delayed with respect to the stimulus and deactivated at negative potentials.

The small transitions labeled * and ☆ usually occurred instantaneously upon application of both positive and negative potentials, while the large transitions (also instantaneous), gathered in current bursts at both positive and negative potentials, look very similar to the FV channel already described by Hedrich and Neher (1987) and to the VK channel studied by Ward and Schroeder (1994). However, contrary to these two channels, our channel did not show any evident calcium dependence (*see* following results and the Discussion section); therefore, we will indicate it with the term FV1 channel. As shown in Fig. 3, the FV1 vacuolar channel was statistically observed in all the patch-clamp configurations tested (whole-vacuole, on-vacuole and excised patch outside-out) without showing any evident voltage dependence (Fig. 5*B*). Since it was very difficult to distinguish the macroscopic voltage-independent currents from the leakage, we decided to investigate the electrical properties of the tonoplast by analyzing single-channel records. Under our experimental conditions, both SV and FV1 channels exhibited a long-lasting activity and occasionally both channels could be observed in the same patch

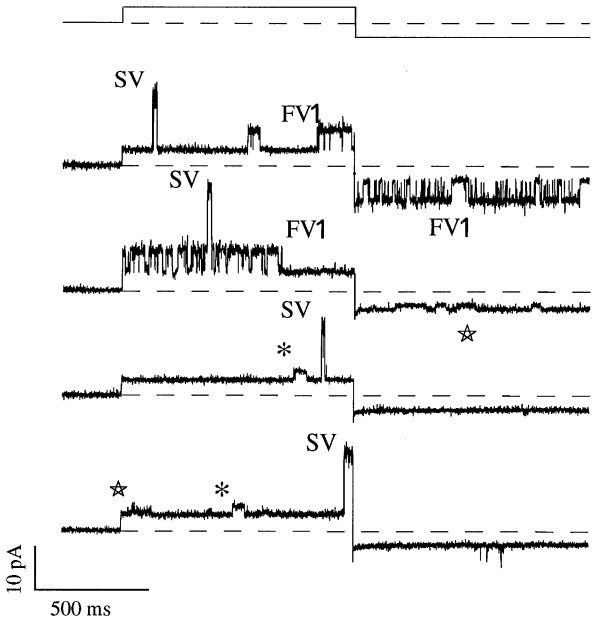

Fig. 2. Vacuolar single-channel openings recorded in outside-out patches. Typical single channels recorded in symmetric KCl 600 mM; other conditions as in standard ionic solutions. Holding and step potentials were 0 and ±50 mV, respectively. Dotted lines mark the zero current level.

(Fig. 3, panel *A* and *B*). Under optimal conditions, they would be easily identified and compared. Evidently, the voltage independent channels can be more easily recognized at negative transmembrane potentials or at relatively low positive potentials where the probability of activation of the SV channels is very low. The long single-channel bursts, that clearly resolved at negative potentials (Fig. 3), are representative of the FV1 channel. This burst-mode is a fingerprint that can be used for identification of FV1 channel type.

Effects of Cytosolic Calcium

Figure 4*A, B* and the Table demonstrate that an increase of the cytoplasmic calcium concentration (from 6 μM to 1 mM) increased the macroscopic SV current (Hedrich & Neher, 1987) as a consequence of an increment of the opening probability of the channel; likewise, (panel *B* and *C*) in nominally zero calcium, the frequency of occurrence of single SV channels decreased with respect to the standard ionic solutions.

With respect to standard solutions, the addition of 1 mM cytoplasmic calcium decreased the single-channel conductance of the outward currents but did not affect the inward current of the SV channel measured from instantaneous tail currents. The amplitude of the outward single SV channel decreased by 25% when the calcium concentration on the cytoplasmic side was increased from 6 μM to 1 mM (in 150 mM KCl); as an example, in standard control solutions at $V = +100$ mV, we measured $I = 11.5 \pm 0.2$ pA (mean ± SEM), while when calcium was increased to 1 mM, the channel amplitude decreased to $I = 8.6 \pm 0.3$ pA; on the other hand, at $V = -100$ mV, the single-channel current was 11.8 ± 0.3 pA and 11.4 ± 0.3 pA in standard control solutions and when Ca^{2+} was 1 mM, respectively.

Alteration in the calcium concentration affected the kinetics of activation but did not affect the deactivation of SV channels. The kinetics of current activation are faster at higher calcium concentrations as $t_{1/2}$ decreased (Fig. 4A) from 1 sec ([Ca] = 6 μM) to 0.4 sec ([Ca] = 1 mM), while the deactivation time, τ_D, (measured stepping from a main pulse of +100 mV to a tail voltage of −100 mV) was equal to 21.9 ± 0.6 msec ($N = 9$) in 6 μM Ca^{2+} and 22.2 ± 0.6 msec ($N = 9$) in 1 mM Ca^{2+}. Therefore calcium ions participate in the regulation of the mechanisms controlling the SV channel activation but they are not involved in the deactivation of this channel.

In the case of the FV1 type channel, an increase of cytoplasmic calcium concentration did not induce any consistent change in the opening probability, measured at potentials of −100 and −40 mV. The Table reports the relative probabilities of the two channels at 0 and 1 mM calcium with respect to our control conditions (i.e., $[Ca^{2+}] = 6$ μM). We also verified that, in the absence of calcium, the voltage independent channel was subjected to a rapid and irreversible rundown, while at μM concentrations of cytoplasmic calcium it was stable (like the SV-type channel) and could be recorded also for one hr. Finally, comparing the single-channel amplitudes obtained in different $MgCl_2$ concentrations, we observed that a symmetric increase of Mg^{2+} (from 2 to 5 mM) caused a decrease (up to 50%) of the single-channel amplitude of the SV and FV1 channel (*not shown*).

Voltage Dependence

By applying a double pulse protocol (Fig. 5*A*) we verified that the current of the two largest (SV and FV1) channels increased linearly with the applied membrane potential. In standard symmetric solutions SV and FV1 channels displayed conductances of 103 ± 2 pS and 41 ± 1 pS, respectively. In Fig. 5*B* the opening probabilities of the two channels are reported as a function of the transmembrane potential. It can be observed that the activation of the FV1 channel did not depend appreciably on the applied membrane voltage. Since the instantaneous single-channel *I-V* characteristics were linear over the entire voltage range analyzed (±100 mV), the rectifying characteristic of the SV channel must be ascribed to a strong voltage dependence of its opening probability. It should be noted that, in order to construct a rapid and

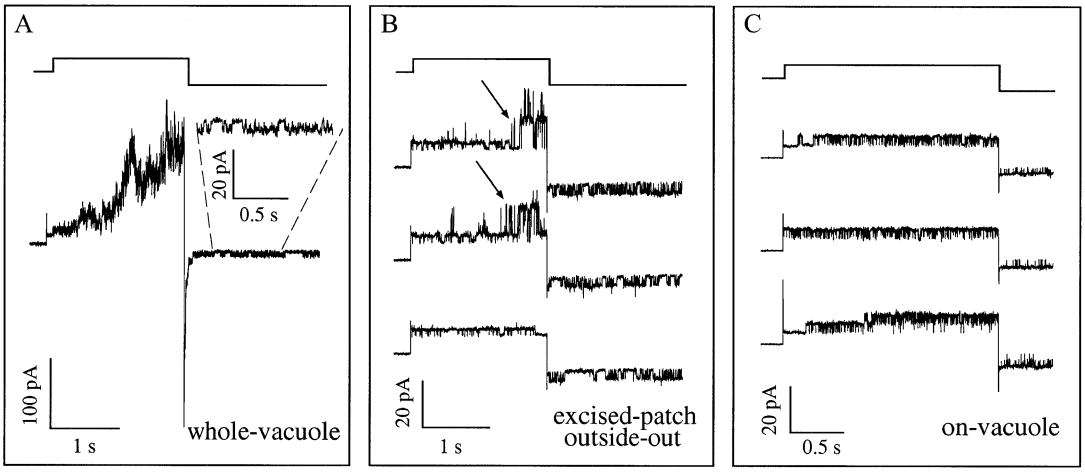

Fig. 3. FV1-type channels were present in all the patch-clamp configurations tested. Bursty FV1-type channels were present in whole-vacuole currents (panel *A*), outside-out excised-patches (panel *B*) and in vacuole-attached patches (panel *C*). (*A*) In the presence of a large component of the slow activating current, FV1 channels can be more easily observed at negative voltages. The inset shows, at higher current and time resolution, the section of the record delimited by the dotted segments. (*B*) Both SV and FV1 type channels were present in this excised patch. Notice the delay in activation and the larger amplitude of the SV channel (indicated by the arrow) present only at positive potentials. (*C*) Two FV1 channels can be identified in this vacuole-attached patch. Holding and step potentials were 0 and ±100 mV, respectively. Standard ionic solutions.

complete current voltage characteristic of the two channels, also at voltages where the SV channel deactivates (*c.f.* Hedrich et al., 1986), the data in Fig. 5 were derived from double pulse voltage protocols. Therefore, pulsed voltage protocols were convenient to identify the vacuolar channels on the basis of their kinetic properties. However, taking advantage of the fact that the vacuolar channels did not inactivate, voltage ramps or continuous voltage stimulations (lasting for several seconds and even minutes at the same voltage) were also applied. These procedures allowed us to perform a more detailed analysis of the time and voltage-dependence of the channel types shown in Fig. 2.

In the voltage range investigated (typically ±100 mV), all the channels identified displayed linear single-channel characteristics. A typical representation of the current as a function of the voltage (in standard solutions) is given in Fig. 6*A;* equivalent results were obtained in standard solutions where symmetric KCl concentrations ranged from 50 mM to 1 M. The linearity of the current-voltage characteristics is also evident when low frequency (1 Hz) voltage ramps were applied (panel *B*). Channel events were systematically identified also on the basis of their kinetic properties. Since the data in Fig. 6 were collected under continuous stimulation protocol, the SV channel characteristic does not show experimental points at negative transmembrane voltages. On the other hand, the voltage-independent channels could be identified because they displayed long current bursts and several openings (gathered together) were interrupted by relatively short closures lasting a few msec. In accordance with the results reported in Fig. 5, from data collected under continuous stimulation protocols, the SV to FV1 single-channel conductance-ratio is approximately 2.5.

Selectivity and Conductance

To obtain more information concerning channel selectivity and a preliminary evaluation on the size of the pores, we performed experiments where cytoplasmic potassium was substituted by the macro-cation tetramethylammonium (TMA), frequently used as an impermeant cation for potassium channels (Hille, 1975; Almers et al., 1984; Fukushima & Hagiwara, 1985; Colombo et al., 1987). We verified that at positive potentials TMA did not permeate through both the SV and FV1 channels (Fig. 7); instead, when the transmembrane potential was inverted, both channels were immediately permeable to lumenal potassium (*see* as an example the middle records in Fig. 7). Under the double pulse protocol, the presence of channel openings at negative voltages confirmed that in 150 mM TMACl the channels were still active and their kinetics did not change. Indeed, SV channels still inactivated in a few msec whereas FV1 channels maintained their bursting characteristic. However, TMA is not a blocker of the vacuolar channel since we verified that the addition of millimolar concentrations of TMACl to the standard bath solution did not affect the channel openings (*not shown*).

Like the macroscopic currents shown in Fig. 1*C,* single channel data (Fig. 8) (collected in asymmetric KCl solutions) representative of the three largest conductances also displayed reversal potentials (~−20 mV) in agreement with the Nernst potential for potassium (−20.2 mV indicated by the arrow in Fig. 8).

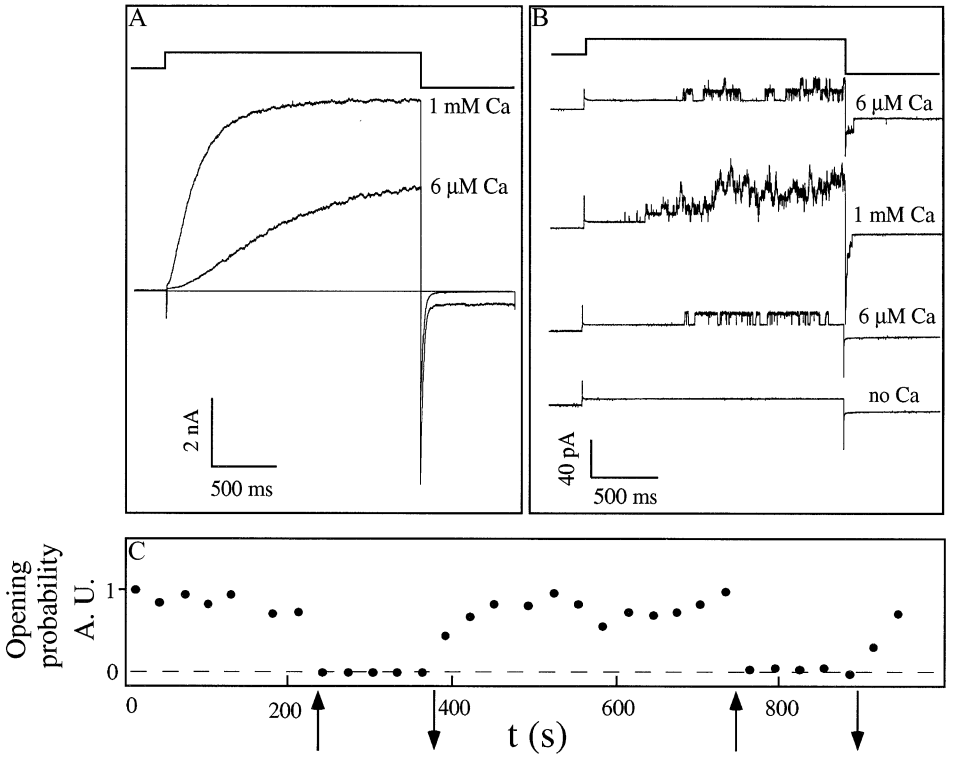

Fig. 4. Cytoplasmic calcium concentration regulates the SV-type channel. (*A*) The macroscopic SV current increased (by a factor of two) increasing the cytoplasmic calcium concentration from 6 μM to 1 mM. Each curve represents the average of seven successive records. (*B*) Single-channel recordings (in excised outside-out patches) at the Ca^{2+} concentrations indicated. In both panels, the upper inset represents the potential protocol: holding, test and tail potentials were 0, +100 and −100 mV, respectively. (*C*) A series of double pulse stimula were applied to the vacuole and the opening probability (in Arbitrary Units) was plotted as a function of the time of the stimulus. Upward arrows indicate the perfusion with zero calcium, i.e., when the standard external solution (containing 6 μM calcium) was replaced by an identical solution which did not contain free calcium (i.e., 1 mM EGTA and no Ca); downward arrows indicate the recovery.

The permeability properties and the conductances of the sugar beet tonoplast channels were studied as a function of the KCl concentration in the range 50 mM–1 M. As an example, Fig. 9 shows that at each KCl concentration the SV-type channel exhibited linear *I-V* characteristics. Similar results were also obtained plotting the current-voltage characteristics of single events corresponding to the other channels identified (*not shown*). A summary of this study is shown in Fig. 10, where the conductances are plotted as a function of potassium activity on a bilogarithmic scale. It can be observed that for all channel types the conductance increased linearly at low KCl concentrations showing a maximum at activities ranging from 250 to 350 mM. Together with selectivity experiments, the increase of the conductance as a function of K^+ concentration unequivocally confirms that under our working conditions the ionic current is mainly driven by potassium ions and that a conductance maximum is present.

Discussion

We have shown that in the sugar beet tonoplast several channel types can be observed together with the SV-type channel. At least three other channels did not show any apparent dependence of the opening probability on the membrane potential. Among the voltage independent channel types, the opening probability of the largest one (FV1) did not depend significantly on the cytosolic calcium concentration (in the micromolar-millimolar range). It ran down in the total absence of external calcium and displayed a single-channel conductance that is about half (1:2.5) the conductance of the SV channel (*see also* Hedrich & Neher, 1987). The kinetics and the selectivity properties, but not the calcium-dependence, of our FV1 channel are comparable to those of the VK channel identified by Ward and Schroeder (1994) in guard cell vacuoles. Indeed, contrary to the VK channel, the opening probability of our FV1 channel was not appreciably affected by the concentration of cytoplasmic calcium (*see* Table). The rundown, which we observed in nominally zero cytosolic calcium, looks different from the calcium regulation of the VK channel because the FV1 channel inhibition was irreversible and therefore may have been caused by denaturation or unfolding of the protein.

We have also shown that the conductance of all the channels present under our experimental conditions in-

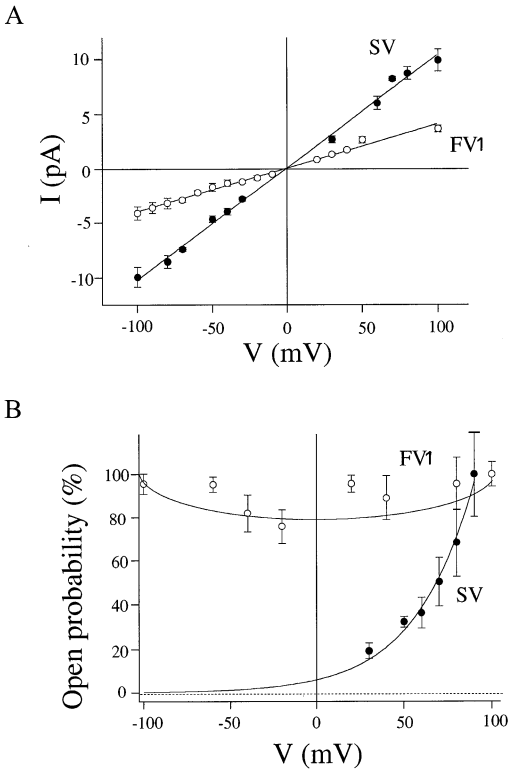

Fig. 5. *I-V* characteristics and opening probability of the two largest channels. (*A*) Single-channel current-voltage characteristics of the FV1 (empty circles) and SV (filled circles) channels obtained from step pulses up to different membrane potentials. Excised patch outside-out. At negative potentials, the current values of the SV type channel were obtained from tail currents before the channel inactivated. Holding potential was 0 mV. (*B*) The opening probability of the two largest channels normalized with respect to the value measured at V = +100 is reported. Data were collected in the on-vacuole configuration; bath and pipette contained the standard solutions. The same symbols as in *A*.

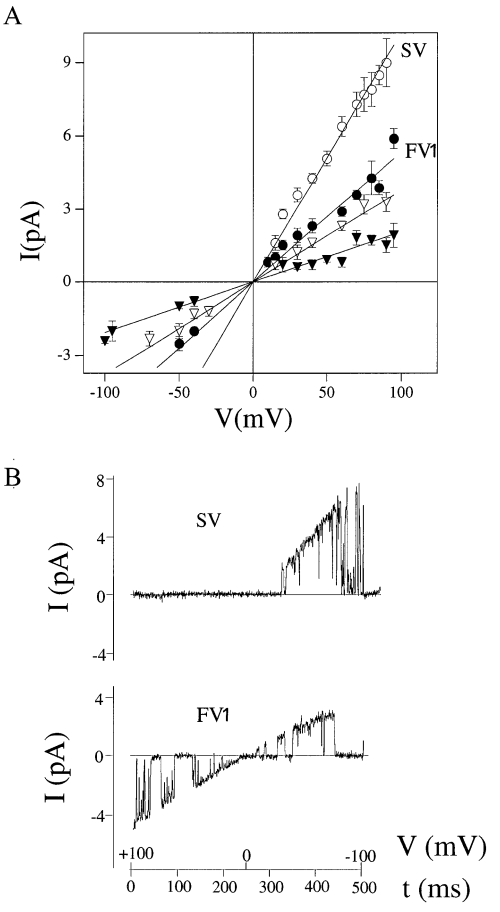

Fig. 6. Current-voltage characteristics of the four current levels identified in sugar beet vacuoles. (*A*) *I-V* characteristics obtained from a systematic single-channel analysis performed on continuous current records. Continuous lines represent the best fit to the experimental data. (*B*) *I-V* characteristics of the SV and FV1 channels obtained changing the membrane potential linearly from −100 to +100 mV over 500 msec. Excised patch outside-out; standard ionic solutions.

creased together with the KCl concentration, thus suggesting that the ionic current is essentially driven by potassium ions (Lado et al., 1989). Moreover, selectivity experiments performed in asymmetric KCl confirmed that at least the three most conductive channels are selective for potassium. Accordingly, using constant field approximation (Lewis, 1979, Eq. 4), we evaluated that, though Mg^{2+} displays high affinity for the SV channel ($P(Mg^{2+})/PK^{+} \approx 1.5$), in our experimental conditions the majority of the current is driven by K^{+} ions while Mg^{2+} contributed to the current for a few percent and up to a maximum of ≈10% (Lewis, 1979) when KCl = 50 mM. These conclusions are also supported by experiments where KCl was replaced with identical concentrations of TMACl: the disappearance (at positive potentials) of all types of transitions when potassium, but not chloride and magnesium, were removed from the bath constitutes a further and direct demonstration that the majority of the current through the two largest channels is due to potassium permeation through the pores. On the other hand, the immediate availability of the inactivating SV channels and of the bursty FV1 channels at negative potentials indicates that TMA did not permeate through the pore owing to its steric hindrance (cristal radius 2.8 Angstrom, Hille, 1975) without blocking the channel permanently. This conclusion is also supported by experiments where millimolar concentrations (up to 5) of TMA, added to the external standard solutions, did not affect the single channel conductance. Therefore, the diameter of the SV and FV1 pores should be smaller than 0.6 nm (Hille, 1975*b;* Hille, 1992; McCleskey & Almers, 1985) and the ion permeation should be regulated by interaction of the permeating ions with the internal walls of the pore.

We also verified that an increase of the cytosolic calcium concentration (from 6 μM to 1 mM) increased the ionic currents of sugar-beet tonoplasts by increasing the opening probability of the SV-type channel, while it had very little effect on the voltage-independent channel

Table. Effects of cytoplasmic calcium on the opening probability of the SV and FV1 channel

$Ca_{cyt.}$	FV1 channel	SV channel
Ca = 1 mM	$P_F(-100\ mV) = 2.2 \pm 1.3$	$P_S(+100\ mV) = 7.2 \pm 2$
Ca = 1 mM	$P_F(-40\ mV) = 1.8 \pm 0.7$	$P_S(+40\ mV) = 125 \pm 93$
Ca = 0 mM	$P_F = 0$	$P_S = 0$

The relative opening probability of the SV and FV1 channel, measured in 1 mM calcium and 0 calcium, normalized with respect to the probability measured at the same potential but under control conditions (6 μM calcium). Note that, as far as the SV channel is concerned, the large values of the probability and SD measured at V = +40 mV are affected by the low frequency of occurrence of the channel at this potential under control conditions. In zero calcium, the opening probability was zero for both channel types at any applied potential. However, note that different causes are responsible for the low conductivity in the absence of calcium: the slow channel completely deactivated, decreasing the calcium concentration, but it also recovered in standard solutions; whereas, the voltage-independent channel, in the absence of calcium, was subjected to a rapid and irreversible rundown. Data were obtained in vacuole-free patches in the outside-out configuration.

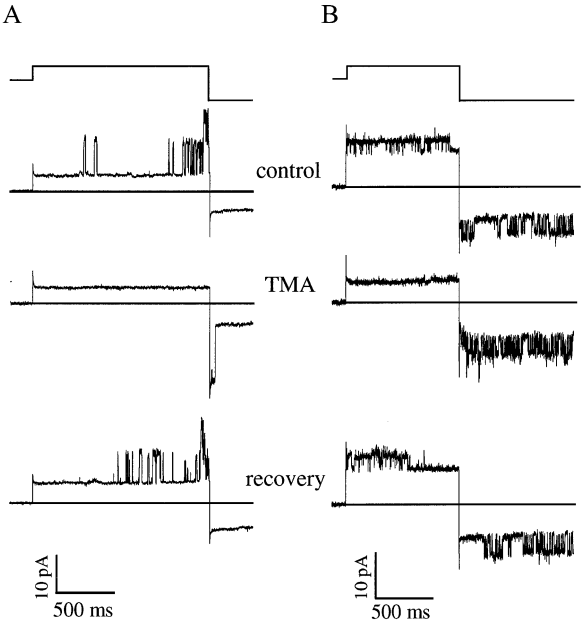

Fig. 7. TMA did not permeate through both SV (panel *A*) and FV1 (panel *B*) channels. In control and recovery the membrane patch was exposed to the external standard solution; when the external 150 mM KCl was replaced with an identical concentration of TMACl, no single-channel openings could be observed at positive potentials. Holding potential 0 mV; test pulses to +80 mV; tail pulses to −100 mV. The perfusion was performed using the fast procedure technique. Single-channel currents systematically disappeared and reappeared during the first test pulse (5-sec interval) following the application of TMA^+ and K^+, respectively. Excised outside-out patches. The pipette contained the standard internal solution.

type. However, 1 mM cytoplasmic calcium decreased (*see also* similar results reported by Ward and Schroeder, 1994) by 25% the single channel conductance of the SV-type channel measured at positive potentials, while it did not affect the amplitude of the same channel (measured before deactivation) at negative potentials. Preliminary observations suggest that Mg^{2+} also decreased the single-channel conductance since in 5 mM $MgCl_2$ the SV and FV1 single-channel conductance is half the conductance in an identical KCl concentration but in 2 mM $MgCl_2$. Moreover, if the cytosolic solution was changed from 100 mM KCl to 50 mM $CaCl_2$, in the presence of millimolar concentrations of KCl in the bath, the macroscopic ionic current mediated by the SV channel was completely abolished. Also, the voltage-independent current decreased significantly, although this decline could not be quantified in detail because in the whole-vacuole configuration this component cannot be easily distinguished from the leakage (*data not shown*).

We suggest that, similar to some classes of Ca^{2+} (Almers & McCleskey, 1984; Hess & Tsien, 1984) and K^+ animal channels (Perez-Cornejo & Begenisich, 1994; Korn & Ikeda, 1995), also vacuolar channels control ion selectivity owing to a competition by rejection mechanism. Therefore, Ca^{2+} and Mg^{2+} enter into the pore (Ward & Schroeder, 1994) of the two major channels of the sugar beet tonoplast, where, according to a multi-ion single file permeation mechanism, they decrease the K^+ current by electrostatic repulsion. The entry of Mg^{2+} into the pore is clearly supported by the shift of the reversal potential observed changing the external Mg^{2+} concentration; this fact also demonstrates that the deviation of the reversal potential from the Nernst potential for K^+ is due to Mg^{2+} and not to Cl^- ions (*see also* Lado et al., 1989). The channels may be permeable both to K^+ and to divalent ions, but the latter have greater affinity as well as a slower permeation (with respect to K^+) through the SV pore. A competition by rejection mechanism was also assumed by Johannes and Sanders (1995) to explain the transport properties of calcium permeable channels in sugar beet vacuole. In our case, the validity of such a mechanism is supported by the good agreement between the Nernst potential for K^+ and the experimental reversal potential of channels shown in Fig. 8. Indeed, the data in Fig. 8 were obtained at a cytosolic K^+/Mg^{2+} concentration ratio 8 times larger with respect to the conditions of Fig. 1*C;* this fact suggests that the SV selectivity may depend on the composition of the ionic solutions as demonstrated by numerical results of flux equations through multi-ion pores in the presence of monovalent (Hille & Schwarz, 1978) and divalent (Campbell et al., 1988) ion mixtures.

Moreover, it has been demonstrated that, for multi-ion-binding single-file diffusion pores, the concentration dependence of the single-channel conductance exhibits a maximum (Hille & Schwarz, 1978). For a symmetrical two-site channel bathed in equal concentrations of the

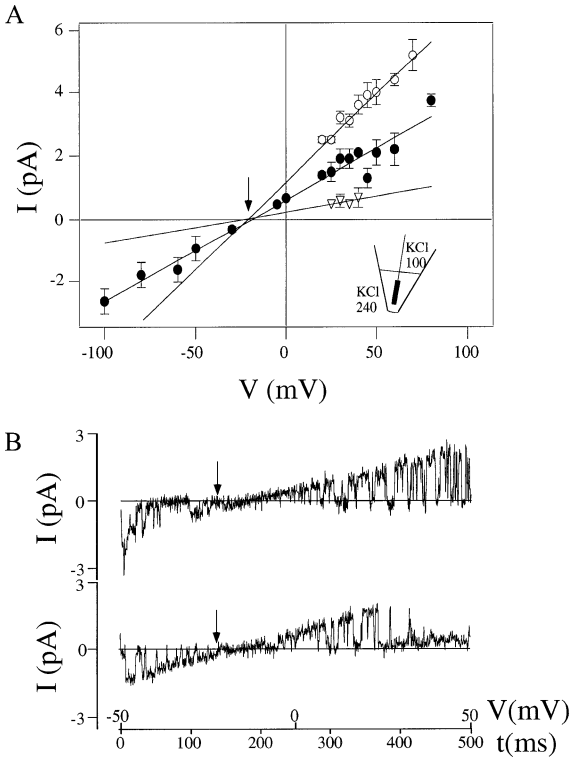

Fig. 8. Single-channel *I-V* characteristic recorded in asymmetric solutions. (*A*) The reversal potentials for the SV (−21 ± 5 mV), FV1 (−19 ± 3 mV) and the smaller channels were in good agreement with the Nernst potential for potassium = −20.4 mV (indicated by the arrow). (*B*) FV1 channel characteristics obtained by a linear variation of the membrane potential are in good agreement with the data collected from continuous potential protocols reported in panel *A*. The membrane potential was changed linearly from −50 to +50 mV over 500 msec. Excised patch outside-out; 100 mM internal potassium (+0.5 mM KOH) and 240 mM external potassium (+6 mM KOH), other conditions according to standard ionic solutions.

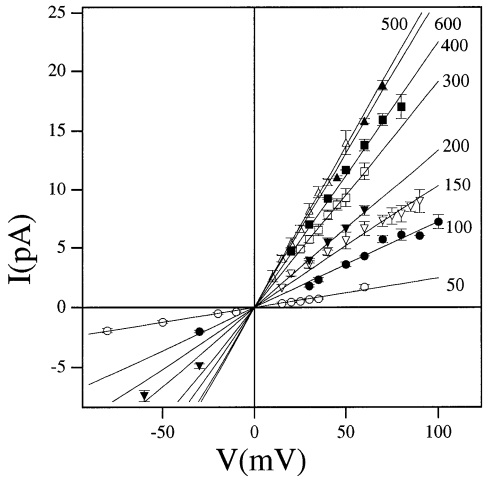

Fig. 9. Single-channel current-voltage relationships of the SV-type channel in KCl concentrations which varied from 50 up to 600 mM, other conditions according to standard ionic solutions. The *I-V* characteristic obtained in symmetric KCl = 1 M was omitted for the sake of clarity. Excised patch outside-out.

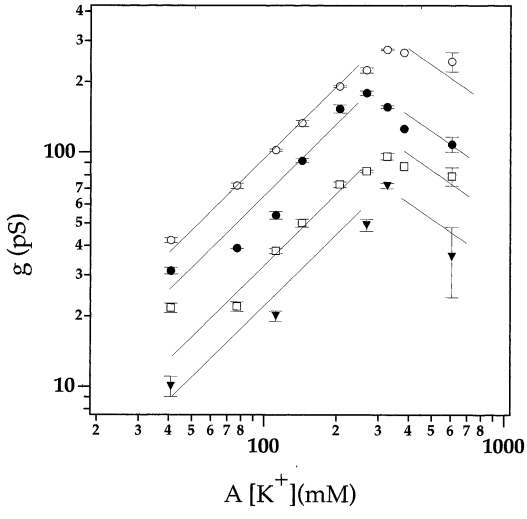

Fig. 10. Single-channel conductances (of the four current levels identified) plotted as a function of K^+ activity on a bilogarithmic scale. Continuous lines represent straight lines with slope 1 and −1.

permeant ion (in our case K^+), the conductance rises with a slope of one as the K^+ activity increases, then the conductance peaks and decreases again with a slope of −1 (Hille & Schwarz, 1978). This trend is clearly represented in Fig. 10 where continuous lines with slopes 1 and −1 were superimposed on experimental data points. A maximum in the conductance and a consequent current decrease at larger K^+ activity is particularly evident for the three smallest channels, while it is less evident in the case of the SV channel type. Unfortunately, owing to membrane instability, it was not possible to study vacuolar channels at KCl concentrations larger than 1 M. We observe that our data are consistent with the results obtained by Schulz-Lessdorf and Hedrich (1995), who simply suggested a linear increase of the SV-single channel conductance up to 300 mM KCl, since they did not study in detail the conductance of the SV channel (in *Vicia faba* and sugar beet vacuoles) at large K^+ concentrations.

A maximum in the conductance of multi-ion pores can be usually observed at high concentrations of the permeating ions because it derives from a complete occupancy of the pore by the permeating ions (Hille & Schwarz, 1978). Accordingly, our vacuolar channels displayed a maximum in the conductance at KCl activity ranging from 250 to 300 mM. On the other hand, the selectivity properties of a multi-ion pore can change at low ionic concentrations (when only one site of the pore is occupied) in correspondence with the anomalous mole fraction effects observed when the ionic current is plotted *vs.* the mole-fraction (Hille & Schwarz, 1978) of two permeating ions. Therefore, changes of the selectivity

properties and a maximum in the conductance are two distinct aspects of a multi-ion-binding single-file diffusion pore, but the first effect can be observed at ionic concentrations much lower than the second one (Hladky & Haydon, 1972; Hagiwara & Takahashi, 1974; Hagiwara et al., 1977; Hess & Tsien, 1984; Korn & Ikeda, 1995).

Since it has already been demonstrated that a multi-ion single-file diffusion mechanism occurs also for other channels of the sugar beet vacuole (Johannes & Sanders, 1995), it can be hypothesized that, during evolution, sugar beets (and possibly other plants) adopted this apparently rough selectivity mechanism to efficiently accumulate and deliver different ions from the vacuole by using a limited number of permeation sites. It is possible that the same channel changes its selectivity properties under different physiological conditions; for example when the ionic solutions inside or outside the vacuole change drastically owing to growth of the plant, water stress or to variations of mineral nutrients in the soil. Since the tonoplast is normally slightly hyperpolarized (−10 to −50 mV), owing to the action of the electrogenic proton pump driving H^+ into the vacuole, the SV channel is normally inactive; however, if for any reason the efficiency of the H^+-pump decreases, the vacuole may depolarize and the SV channel may start to cooperate with the pump to buffer the transmembrane potential by means of an influx of K^+ into the vacuole. Other ions, including divalent ions, can also be transported into the vacuole if their local concentration increases atypically at the membrane interface. We observe that the SV channel is the tonoplast channel most sensitive to the external calcium concentration. As a consequence, under stress conditions, an increase of the local calcium concentration may activated the SV channel which will eventually drive potassium or even calcium (if this ion is prevalent) into the vacuole. On the other hand, it is difficult to quantify the percentage of the total current which is due to the voltage-independent channels, because in whole-vacuole configuration their contribution cannot be easily distinguished from the leakage current. Presumably, under normal conditions, they play a central role in regulating the ion distribution because channels other than the SV type are usually open at both negative and positive transmembrane potentials; therefore, under normal resting conditions, they may help to extrude potassium from the vacuole as well as (being multi-ion pores) other cations. If the vacuole depolarize the voltage-independent channel will possibly cooperate with the SV channel driving cations inside the vacuole.

We tend to exclude that the smaller instantaneous channels characterized in this work may coincide with the calcium-selective (but also potassium-permeable) channels already described in the sugar beet tonoplast (Johannes & Sanders, 1995) because these channels are blocked by submillimolar concentrations of cytosolic calcium. We are currently investigating whether some of the different conductance levels may be due to distinct conformations of the same protein or to immature (but functional) proteins for which the expression is regulated by plant maturation. The fact that all four current levels characterized in this paper have a similar dependence of the conductance as a function of the potassium concentration supports this possibility.

The collaboration by M. Pisciotta and A. Ciavatta in the analysis of some experiments was greatly appreciated. We thank H. Bush and R. Hedrich for their comments to the manuscript. We acknowledge the valuable technical assistance of G. Gaggero and D. Magliozzi and the linguistic revision by T. Agneessens. Research supported by the National Research Council of Italy, Special Project RAISA, subproject N. 2.1 paper N. 2793. F. Stragapede is on a fellowship from Eridania Z.N. Genoa, Italy.

References

Almers, W., McCleskey, E.W. 1984. Nonselective conductance in calcium channels of frog muscle: calcium selectivity in a single-file pore. *J. Physiol.* **353:**585–608

Almers, W., McCleskey, E.W., Palade, P.T. 1984. A nonselective cation conductance in frog muscle membrane blocked by micromolar calcium ions. *J. Physiol.* **353:**565–583

Bertl, A., Blumwald, E., Coronado, R., Eisenben, R., Findlay, G., Gradmann, D., Hille, B., Köhler, K., Kolb, H.A., MacRobbie, E., Meissner, G., Miller, C., Neher, E., Palade, P., Pantojia, O., Sanders, D., Schroeder, J.I., Slayman, C., Spanswick, R., Walker, A., Williams, A. 1992. Electrical Measurements on Endomembranes. *Science* **258:**873–874

Bezanilla, F. 1985. A high capacity data recording device based on a digital audioprocessor and a video cassette recorder. *Biophys. J.* **47:**437–441

Campbell, D.L., Rasmusson, R.L., Strauss, H.C. 1988. Theoretical study of the voltage and concentration dependence of the anomalous mole fraction effect in single calcium channels—New insight into the characterization of multi-ion channels. *Biophys J.* **54:**945–954

Colombo, R., Lado, P., Peres, A. 1987. A hyperpolarization-activated K^+ current in isolated vacuoles of *Acer pseudoplatanus. In:* Plant Vacuoles. B. Marin, editor. pp. 51–56. Plenum, New York

Coyaud, L., Kurkdjian, A., Kado, T., Hedrich, R. 1987. Ion channels and ATP-driven pumps involved in ion transport across the tonoplast of sugar beet vacuoles. *Biochim. Biophys. Acta* **902:**263–268

Fabiato, A., Fabiato, F. 1979. Calculator programs for computing the composition of the solutions containing multiple metals and ligands used for experiments in skinned muscle cells. *Journal de Physiologie* **75:**463–505

Fukushima, Y., Hagiwara, S. 1985. Currents carried by monovalent cations through calcium channels in mouse neoplastic B lymphocytes. *J. Physiol.* **358:**255–284

Hagiwara, S., Miyazaki, S., Krasne, S., Ciani, S. 1977. Anomalous permeability of the egg cell of a starfish in K^+-T1-mixtures. *J. Gen. Physiol.* **70:**269–281

Hagiwara, S., Takahashi, K. 1974. The anomalous rectification and cation selectivity of the membrane of a Starfish egg cell. *J. Membrane Biol.* **18:**61–80

Hedrich, R., Flügge, U.I., Fernandez, J.M. 1986. Patch-clamp studies of ion transport in isolated plant vacuoles. *FEBS Lett.* **204:**228–232

Hedrich, R., Neher, E. 1987. Cytoplasmic calcium regulates voltage-dependent ion channels in plant vacuoles. *Nature* **329:**833–836

Hess, P., Tsien, R.W. 1984. Mechanism of ion permeation through calcium channels. *Nature* **309:**453–456

Hille, B. 1975*a*. Ionic selectivity, saturation and block in sodium channels—a four barrier model. *J. Gen. Physiol.* **66:**535–560

Hille, B. 1975*b*. Ionic selectivity of Na and K channels of nerve membrane. *In:* Membranes—A Series of Advances, Vol. 3: Lipid Bilayers and Biological Membranes: Dynamic Properties. G. Eisenman, editor. pp. 255–323. Marcel Dekker, New York

Hille, B. 1992. Ionic Channel of Excitable Membranes, Sinauer. Sunderland, MA

Hille, B., Schwarz, W. 1978. Potassium channels as multi-ion single-file pores. *J. Gen. Physiol.* **72:**409–442

Hladky, S.B., Haydon, D.A. 1972. Ion transfer across lipid membranes in the presence of gramicidin A. *Biochim. Biophys. Acta* **274:**294–312

Johannes, E., Brosnan, J.M., Sanders, D. 1992. Parallel pathways for intracellular Ca^{2+} release from the vacuole of higher plants. *The Plant J.* **2:**97–102

Johannes, E., Sanders, D. 1995. Lumenal calcium modulates unitary conductance and gating of a plant vacuolar calcium release channel. *J. Membrane Biol.* **146:**211–224

Kolb, H.A., Köhler, K., Martinoia, E. 1987. Single potassium channel in membranes of isolated mesophyll barley vacuoles. *J. Membrane Biol.* **95:**163–169

Korn, S.J., Ikeda, S.R. 1995. Permeation selectivity by competition in a delayed rectifier potassium channel. *Science* **269:**410–412

Lado, P., Colombo, R., Cerana, R. 1989. K^+ channels in the tonoplast of *Acer pseudoplatanus* cells. Plant membrane transport: the current position. J. Dainty et al. editors. pp. 179–194. Elsevier.

Lewis, C.A. 1979. Ion-concentration dependence of the reversal potential and the single-channel conductance of ion channels at the frog neuromuscular junction. *J. Physiol.* **286:**417–445

Maathuis, F.J.M., Prins, H.B.A. 1991. Inhibition of inward rectifying tonoplast channels by a vacuolar factor: physiological and kinetic implications. *J. Membrane Biol.* **122:**251–258

McCleskey, E.W., Almers, W. 1985. The Ca channel in the skeletal muscle is a large pore. *Proc. Natl. Acad. Sci. USA* **82:**7149–7153

Neher, E. 1992. Correction for liquid junction potentials in patch clamp experiments. *Methods Enzymol.* **207:**123–131

Pantoja, O., Gelli, A., Blumwald, E. 1992. Voltage-dependent calcium channels in plant vacuoles. *Science* **255:**1567–1570

Perez-Cornejo, P., Begenisich, T. 1994. The multi-ion nature of the pore in *Shaker* K^+ channels. *Biophys. J.* **66:**1929–1938

Robinson, R.A., Stokes, R.H. 1959. Electrolyte Solutions. Butterworths Scientific Publications, London

Schulz-Lessdorf, B., Hedrich, R. 1995. Protons and calcium modulate SV-type channels in the vacuolar-lysosomal compartment-channel interaction with calmodulin inhibitors. *Planta.* **1971:**655–671

Ward, J.M., Schroeder, J.I. 1994. Calcium-activated K^+ channels and calcium-induced calcium release by slow vacuolar ion channels in guard cell vacuoles implicated in the control of stomatal closure. *Plant Cell* **6:**669–683